

## A hierarchical framework for holistic optimization of the operations of district cooling systems

Zhonglin Chiam<sup>a,b</sup>, Arvind Easwaran<sup>b,\*</sup>, David Mouquet<sup>c</sup>, Samira Fazlollahi<sup>a</sup>, Jaume V. Millás<sup>d</sup>

<sup>a</sup> Veolia City Modeling Centre (VECMC), 23 Pandan Avenue, Singapore 609389, Singapore

<sup>b</sup> School of Computer Science and Engineering, Nanyang Technological University, 50 Nanyang Avenue, Singapore 639798, Singapore

<sup>c</sup> Veolia Environnement Recherche et Innovation (VERI), 291 Avenue Dreyfous Ducas, 78520 Limay, France

<sup>d</sup> Ecoenergies, Carrer Número 27, 6, 08040 Barcelona, Spain

### HIGHLIGHTS

- Framework for the holistic optimization of the hourly operation of district cooling systems.
- Simultaneous optimization of flow and temperature variables, while respecting non-linearities.
- Application of the framework on a case study for illustration purposes.
- Discussion of solutions which resulted in electricity savings of up to 31% across the three cases.

### ARTICLE INFO

**Keywords:**  
 District cooling systems  
 Operation  
 Hierarchical  
 Optimization  
 Mixed integer linear program  
 Genetic algorithm

### ABSTRACT

The potential for greater energy efficiency gave rise to the popularity of implementing district cooling systems. In newer districts, however, the discrepancy between the designed capacity of the cooling system and actual cooling demand usually negates these benefits. In such scenarios, the optimization of the system's operations with respect to cooling demand could considerably improve the energy efficiency of the system, without incurring additional capital costs.

Components of a district cooling system are usually operated at pre-defined setpoints or individually optimized, without regard of the impact on the overall system. Formulation of an optimization problem which adequately captures the thermal and physical interactions as well as the tight coupling between components, i.e., holistically, results in a mixed integer non-linear program which is large and difficult to solve. In this article, a hierarchical optimization framework for the hourly operation of district cooling systems is introduced to manage the problem. The initially complex model of the system was abstracted so that it could be solved effectively using the combination of a genetic algorithm and mixed integer linear program. The mixed integer linear program reduced the search space of the genetic algorithm, thereby increasing the likelihood of achieving global optimality.

Finally, the methodology was applied to a case study based on an existing district cooling system in Europe for illustrative purposes. For the scenarios defined, the thermal and physical variables for each component were tuned such that the hourly cooling demand could be fulfilled with minimal electricity consumed. Results indicate potential electricity savings of up to 31%. At the optimum, some components operated less efficiently for the benefit of the overall system, further reinforcing the advantage of performing optimization holistically.

### 1. Introduction

Issues such as global warming, energy security, and sustainability have led to many initiatives spanning from the adoption of alternative energy to ways of utilizing it more efficiently. As of 2015, the world's total consumption of energy stands at slightly above 9 million tonnes of

oil equivalent (Mtoe), a rise of above 50% from a decade ago [1]. Of which, above 85% of this consumption were derived from non-renewable sources such as coal, oil and gas [2]. This has contributed to increased levels of CO<sub>2</sub> emissions which accelerates climate change [3].

The demand for space cooling accounts for a significant portion of energy demand. This statistic is even more valid in regions experiencing

\* Corresponding author.

E-mail address: [arvinde@ntu.edu.sg](mailto:arvinde@ntu.edu.sg) (A. Easwaran).

significant periods of tropical climates [4]. The percentage of energy used for space cooling in Mumbai (40%) is doubled that of London (20%) [5,6]. District cooling systems (DCS) represent one such example of a potentially more efficient means of fulfilling this demand [7]. Thus, DCS are rapidly becoming a standard feature in new city developments [8,9]. The performance in reality, however, is uncertain as operating and design conditions differ [10]. The tendency to exercise caution in design often leads to the oversizing of DCS; this results in the underutilization of equipment which is especially detrimental to the overall energy efficiency of the system [11,12].

Inefficiency is further compounded by control strategies which are either based on predefined setpoints or seek only to achieve optimal performance, local to components [13,14]. Localized control disregards the cascading effect on the system which inhibits the ability of DCS to adapt well under less-than-ideal operating conditions. The focus of the current work is to introduce an optimization framework which thoroughly explores the solution space mapped by tuneable variables in a DCS, in search of improving energy efficiency holistically at the system level.

### 1.1. District cooling system (DCS)

A DCS is a centralized method of cold thermal energy production and distribution for space and process cooling. Chilled water is widely used as the medium for the transportation of thermal energy for cost-effectiveness [15]. The technical description of a typical DCS is comprised of four main components - the central station, distribution network, customers and heat rejection system. Fig. 1.1 illustrates the general components of a typical DCS serving four buildings. Cooling towers often serve as the primary equipment used for heat rejection. The active components of the DCS which consume electricity are the chillers, pumps and cooling towers. The rate at which electricity is consumed is dependent on the equipment loading, temperature and flowrate setpoints.

### 1.2. Objectives and contributions

For the results of optimal DCS operation to be useful, two criteria must be met. Firstly, the problem formulation needs to be expressed in terms of tuneable variables such as chilled water flowrates and

temperature setpoints. The same cooling demand could be satisfied by various combinations of chilled water flowrates and temperature settings, each impacting efficiency differently. Secondly, it is of utmost importance to capture dynamics of the tight coupling amongst DCS components, while performing optimization holistically. A myriad of non-linearities exists in the governing equations for these components (chiller, pump, cooling towers), making component-level optimization overly naive.

Formulation of the desired optimization problem firstly required the identification of appropriate models for the representation of each component in the DCS. After that, a procedure was introduced to map the interactions between these component models systematically. Binary variables were introduced to enable ‘activation’ and ‘deactivation’ of individual components. The eventual result was a mixed integer non-linear program (MINLP) which is considerably large and challenging to solve.

The hierarchical optimization framework for the holistic optimization of DCS operation was developed for managing the MINLP. It decomposes the optimization problem into two levels – a master and a slave. The key features of the master and slave levels are the genetic algorithm (GA) and mixed integer linear program (MILP) solver respectively. This approach functions by having the GA parameterize a subset of variables such that the remaining could be dealt with using the MILP. Given that MILP solvers generally both converge optimally and more quickly than GAs, an abstraction process was embarked on to linearize the DCS model as much as possible. Doing so, also reduces the load on the GA, promoting resolution speeds and the likelihood of deriving solutions that are globally optimal.

For illustrative purposes, this framework was applied to a case study based on an existing DCS in Europe. Three scenarios, each with different cooling demand and weather conditions, were defined to demonstrate and quantify the potential electricity savings through the application of the proposed framework. Results indicate electricity reduction of 31%, 27% and 3% across high, moderate and low cooling demand conditions respectively.

The proposed optimization framework for DCS and its subsequent application on an existing site are the two main contributions of this paper.

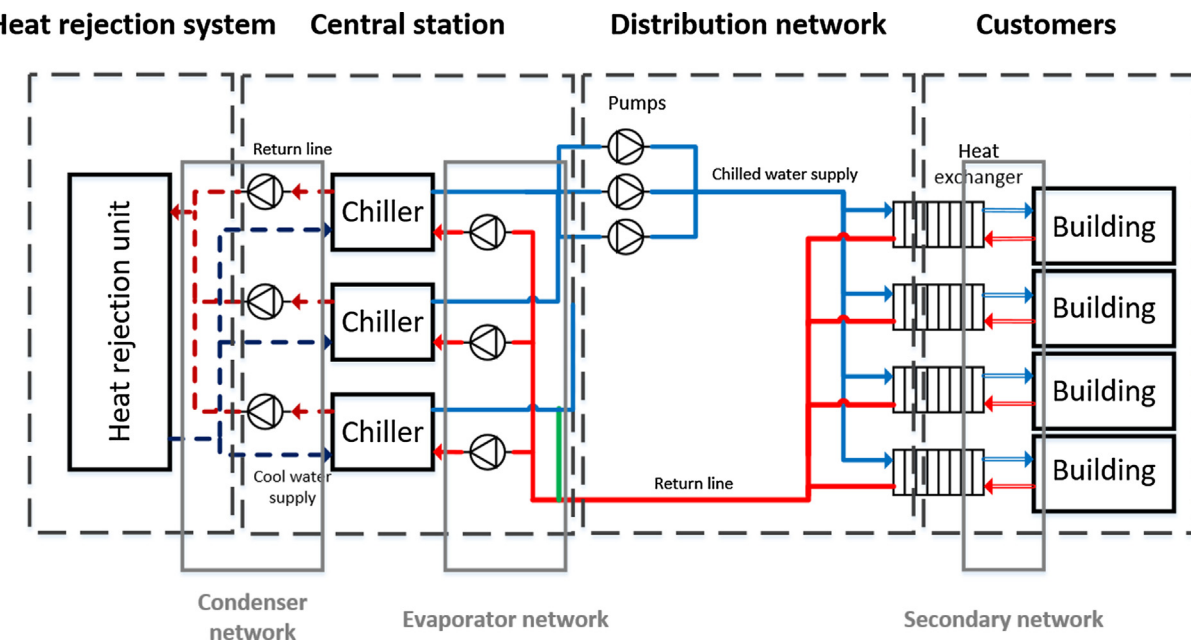


Fig. 1.1. Overview of the components of a typical DCS.

### 1.3. Prior work

Majority of the optimization work done on DCS and closely related district heating systems (DHS) are focused on presenting solutions to design-related issues [15,16]. Such problems attempt to determine the optimal configurations of equipment type, primary resource, network layout, and customer configurations. They employ methods and models which are too abstract for optimizing DCS operations - an example would be the assumption of constant efficiencies, regardless of equipment loading [17,18]. Conversely, optimization of DCS operation is concerned with determining the most efficient equipment staging, flowrate and temperature settings which fulfills a given cooling demand [19,20]. Thus, greater modeling detail of components is required.

Component-level optimization is commonplace where DCS operations are concerned. For a given cooling demand, these formulations attempt to determine the optimal operating plan for equipment [19] and the distribution network [20] separately. Detailed modeling of equipment and network hydraulics involved complex equations, which yields mixed integer non-linear programming (MINLP) problem formulations making the use of meta-heuristics a popular choice [21,22].

Several measures were employed to enhance the solvability of the above component-level optimization problems. Sakawa et al. [23] relaxed the cooling demand constraint by reflecting the failure to meet demand as a penalty in the objective function. With the use of appropriate equation-based models, the MINLP could be broken down into simpler quadratic programs (QP), under the assumption that the set of chillers could be aggregated as a single optimal unit [19]. If the distribution network is extensive, the energy expended for pumping could significantly affect the overall system performance. The relatively small working temperature range further compounds the impact for DCS [24]. To simplify the network optimization problem, Schweiger et al. [20] decomposed the MINLP problem into a mixed integer quadratically-constrained program (MIQCP) and a smaller non-linear program (NLP). This approach reduced the non-convex search space while enabling models of higher detail and physical accuracy to be considered in the problem formulation.

There is no indication that the independent optimization of equipment and network will yield the optimal performance at the system-level. Thus, Jing et al. [21] modeled and optimized the operation of a small-scale district heating and cooling (DHC) system with the consideration of both equipment and network. The formulation enabled the power incurred by the pumps in the network to be reflected in the objective function. However, the direct application of the group search optimizer (GSO) algorithm, does little to ensure the quality of the final solution.

Work on building level optimization of chiller systems were also considered due to their relevance [25,26]. They, however, tend to mainly focus on solving ‘optimal chiller loading’ (OCL) problems, with little regard for the details of the network, nor the setpoint temperature of chillers. Due to the differences in scale of a DCS compared to the building level, the energy expended in the network has to be factored. The benefits of holistic system optimization were highlighted in a case study conducted on a building-level chiller plant, where an additional 6.5% of energy savings was possible on top of chiller-only optimization [27].

From the review, it is evident that there is a lack of studies which consider the holistic optimization of DCS operation, much less a systematic framework for this undertaking. Several studies on the closely related topic at the building level, consider fixed temperature setpoints of chillers, effectively misrepresenting the solution space. For a chiller-based system, the concurrent optimization of temperature setpoints and flowrate in response to a given cooling demand proved to be most effective in the minimization of electricity consumption [28]. DCS are also likely to benefit more profoundly from the consideration of temperature variables as it introduces flexibility into an inherently rigid system. Hence, the novelty of the current work lies in the introduction

of a framework which can simultaneously optimize all tuneable variables of a DCS for a given cooling load.

### 1.4. Organization of the paper

The next section introduces the framework for optimizing the operations of a DCS. Section 3 discusses the selected models and the concomitant abstraction techniques applied, for the compatibility with the framework. Subsequently, the mathematical formulation of the case study based on an existing DCS is presented. Finally, the results of the case study are analyzed and discussed. The purpose of the case study is to validate and illustrate the capabilities of the framework.

## 2. Optimization framework

Taking reference from the approach used by Fazlollahi et al. [16] on DHS, an optimization framework for DCS is proposed in this section. The decomposition method used is the core of the framework. It is introduced to deal with non-linearities in the optimization problem.

It will be apparent from the issues on model abstraction, highlighted in the next section that a method is required to deal with variables which are treated as parameters. MILP can only partially solve the problem. As such, the decomposition approach is employed to couple the MILP formulation with a meta-heuristic based on a GA. The purpose of the meta-heuristic is to handle variables which the MILP solver cannot. It treats the MILP formulation as a more substantial ‘black-box’ to be optimized. This approach is also beneficial to meta-heuristics - having the MILP formulation handle most of the variables reduces the search space, improving solution quality whilst increasing resolution speed as compared to the direct application of the GA. MILP was chosen due to its widespread application in related problems [22].

Fig. 2.1 illustrates the overview of the proposed optimization framework. Details of each aspect in the framework (Pre-processing to post-processing phases) are elaborated in Sections 2.1,2.4. Nomenclature of terms used in this paper are detailed in Table 2.1.

### 2.1. Pre-optimization

The nature of the problem and available data influenced the choice of optimization approach and algorithms. This phase encompasses the preparatory work required for the formulation of the optimization problem, which includes the definition of the objective function, data management, model construction and development of a benchmark. Data management includes two significant aspects - data pre-processing and structuring. Data structuring refers to the organization of data such that easy translation into the form required by the optimization solver was possible. A simulation model comprising the chosen abstracted models is used to benchmark against the ‘optimal’ solutions. For DCS operation optimization problems, the current operational practices are input into the developed simulation model to generate results which are then compared. It also serves as an initial solution for the GA, such that the ‘optimal’ solution generated will always be better than or equal to the benchmark.

### 2.2. Master level

The GA is used at this level owing to its popularity for solving such problems. This algorithm is utilized to handle non-linear variables, which were treated as parameters for the feasibility of MILP formulations.  $T_{\text{evap}}^{\text{in}}, T_{\text{cond}}^{\text{in}}$ , are examples of these variables in the abstracted chiller model Section 3.1. This subset of variables had to be treated as parameters at the slave level, such that the remaining ones can be linearized. The GA is a population-based global search algorithm and could be implemented in several ways.

The task of evaluating the fitness of the selected agents consumes the most time, because it involves the model reduction, solving the

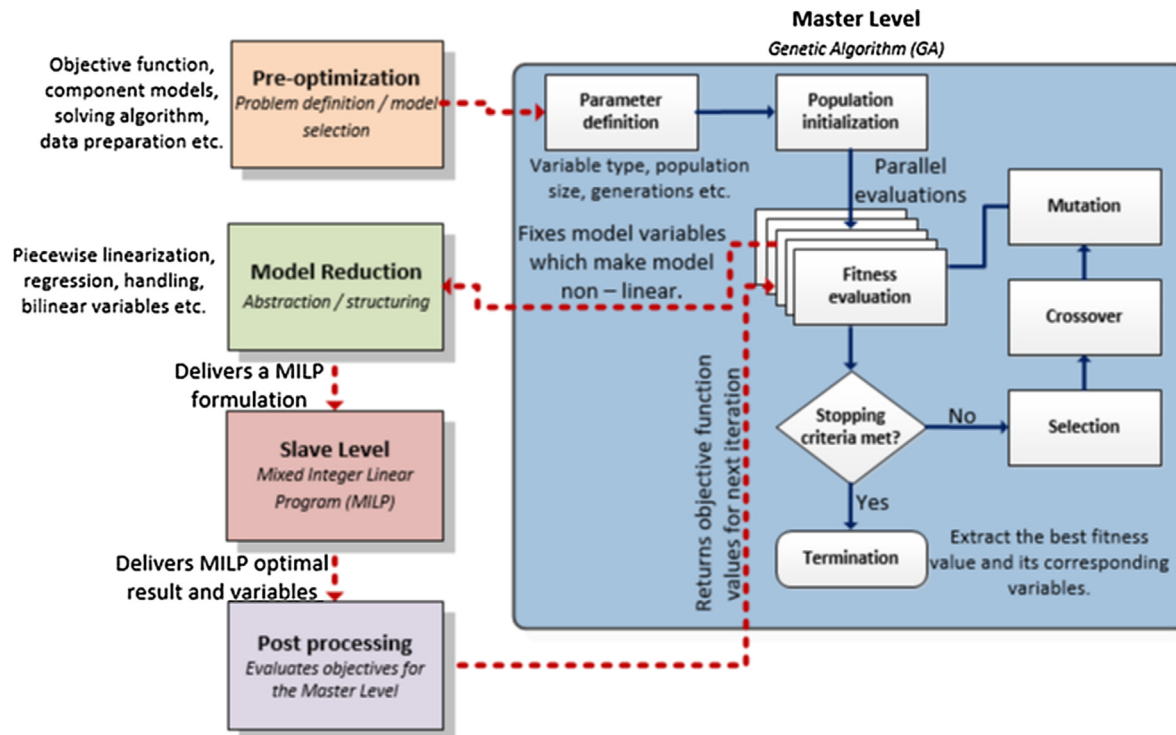


Fig. 2.1. Overview of the optimization framework.

MILP and post-processing steps which makes up the bulk of the framework. Slight modifications were made to the implementation, to improve the speed of convergence. They are the binarization of GA variables and parallelization of fitness evaluations.

### 2.3. Model reduction

Inputs from the master level are required for model abstraction phase. These inputs are GA variables which contributed to non-linearities in the models and hence will function as parameters in the subsequent phases. Details of model abstraction techniques will be discussed in Section 3. The purpose of the abstraction process is to reduce the complexity of the chosen models and facilitate the structuring of data into MILP formulations.

This section focuses on describing the structure defined at the pre-optimization stage for generating a MILP formulation from general bilinear equations. Three building blocks are defined to facilitate the MILP formulation - unit, layer, and constraint.

#### 2.3.1. Unit definition

The unit is defined to represent a component of the DCS (chiller, pump, cooling tower). It comprises at least two continuous MILP variables (up to bilinear), some of which contribute to the objective function value. These MILP variables are constrained by equations describing its capacity and relationship with the other units (streams). Table 2.2 summarizes the unit definition. In the case of the chiller model (Section 3.1) for instance,  $\dot{m}_{evap}$  and  $T_{evap}^{out}$  are variables in the unit definition to be optimized by the MILP. The values of  $\alpha_i$ ,  $\beta_i$  and  $\gamma_i$  are computed using inherent model parameters and GA variables. After which, the contribution to objective function ( $\dot{E}$ ) and stream ( $T_{cond}^{out}$ ) represented by  $y$  and  $z_i$  respectively could be determined.

The bilinear equations in Table 2.2 were linearized using RLT.

#### 2.3.2. Layer definition

Layers are introduced to ‘connect’ the ‘streams’ flowing in and out of units. For DCS, three stream types are defined - fluid, temperature, and

pressure flows. Ideally, equality constraints in the form of  $z_{unit,1}^{out} = z_{unit,2}^{in}$  should be used to respect continuity equations. However such constraints resulted in difficulty for the GA to find feasible solutions. Inequalities are used to rectify the issue. If the inequalities were implemented correctly, the optimal solution would never violate continuity equations as a sub-optimal solution would entail. On occasions where the variables in the GA result in a feasible MILP formulation which violated continuity laws, a penalty function is imposed to reflect the extent of violation to the objective function of the GA. This penalty function is selected to be smaller than the penalty of infeasibility and acted as a guide for the GA to eventually converge to a feasible solution. Table 2.3 describes the three layer types defined in the DCS framework.

#### 2.3.3. Constraint definition

This feature is added to accommodate the need for additional constraints onto the problem formulation. Constraints could be of any form. The two commonly used ones are loosely termed as ‘unit-use’ and ‘stream-limit’ constraints. The ‘unit-use’ constraint serves the purpose of imposing a limit on the number of units activated. ‘Stream-limit’ constraints are introduced to limit the in and outflows of ‘units’.

### 2.4. Slave level and post processing

The MILP sub-problem is solved in the slave level using Gurobi [29]. The optimal solution to the sub-problem is then post-processed before returning to the master level. Post processing included the communication of various levels of infeasibilities and conversion from RLT back to the original variable forms.

## 3. Model selection and abstraction of DCS components

Selected models of commonly found components in DCS and their accompanying abstraction procedure are detailed in this section. Equation-based models are preferred because they are relatively accurate and properties of these equations give insight into the ‘class’ which the resulting optimization problem might fall in. Linearization of these

**Table 2.1**  
Nomenclature of terms used.

Symbol (unit)	
$C_p$	specific heat of the working fluid, (kJ/kg K)
$COP$	coefficient of performance
$\dot{E}$	electricity consumption, (kWh)
$\dot{m}$	mass flowrate of the working fluid, (kg/s)
$\Delta P$	pressure difference, ( $mH_2O$ )
$\Delta T$	temperature difference (K)
$F$	capacity constraints, limits
$T$	temperature, (K)
$\dot{Q}$	thermal energy flow, (kWh)
$R^2$	coefficient of determination
$x, y, z$	generic variables
$Y$	binary on-off variable
%	percentage
<b>Greek letters</b>	
$\alpha, \beta, \gamma, \nu$	regression-derived coefficients
$\varepsilon$	heat exchanger efficiency
<b>superscript</b>	
$in$	flow entering the unit
$out$	flow leaving the unit
$min, max$	upper and lower limits of a defined unit
<b>subscript</b>	
$air$	air, natural/inducted through cooling tower
$approach$	the approach temperature of the cooling tower.
$br$	parallel branch
$cond$	condenser side of the chiller
$cp$	common pipe/decoupler, a feature of primary-secondary pumping configuration
$ct$	cooling tower
$ch$	chiller
$db$	thermodynamic dry-bulb
$DCS$	district cooling system
$demand$	the cooling demand of the $i^{th}$ customer
$dist\_nwk$	distribution network
$ep$	evaporator common exit pipe
$evap$	evaporator side of the chiller
$evap\_nwk$	evaporator network
$fr$	fluid flowrate
$i, m, n, 1, 2, etc.$	numerical labels
$limit$	upper limit of substation ‘cold-side’ temperature difference/supply temperature
$mu$	make-up water
$operating$	operating point of a given pump-system configuration
$out$	flow leaving the unit
$p$	pump
$sel$	equivalent pump selected
$slave$	slave level
$shared$	shared section of the evaporator network
$sys$	evaporator/distribution network system
$ss$	substation
$unit$	generic DCS component
$wb$	thermodynamic wet-bulb
//	parallel network

equation-based models enables the MILP solver to optimize more variables than otherwise possible, which is essential for the solvability of the problem. All chosen models were formulated with the objective of minimizing total electricity cost.

### 3.1. Chiller

Chillers are the core component of an overwhelming majority of DCS. They produce cooling by extracting and rejecting heat at the evaporator and condenser respectively. The objective of this model is to map the relationship between the temperature and flowrate variables on both the evaporator and condenser sides of the chiller to the electricity consumption.

Gordon-Ng universal chiller model (GNU) was selected to represent the required relationship [30]. It is a quasi-empirical model, and thus

could be calibrated with raw data. The model incorporated laws of thermodynamics and energy balances at heat exchangers with some assumptions of internal and external energy losses. As a result, it displayed relatively good predictive capabilities (including extrapolation) despite limited data points [31,32].<sup>1</sup>

Eq. (3.1) is the describing equation for the GNU model. Using the GNU model together with the COP definition and steady-flow energy equation (SFEE) on the evaporator and condenser sides (Eqs. (3.2)–(3.5)), the electricity consumed by the chiller could be expressed in terms of the temperatures and flowrates on both sides of the chiller. A coefficient  $\alpha_0$  was added to Eq. (3.5) so that it could be calibrated using raw data.

$$\frac{T_{evap}^{in}}{T_{cond}^{in}}(1 + \frac{1}{COP}) - 1 = \beta_0 \frac{\dot{Q}_{evap}}{\dot{Q}_e} + \beta_1 \frac{T_{cond}^{in} - T_{evap}^{in}}{T_{cond}^{in} \dot{Q}_{evap}} + \beta_2 \frac{\dot{Q}_{evap}}{T_{cond}^{in}}(1 + \frac{1}{COP}) \quad (3.1)$$

$$COP = \frac{\dot{Q}_{evap}}{\dot{E}_{ch}} \quad (3.2)$$

$$\dot{Q}_{evap} = \dot{m}_{evap} \times C_p \times (T_{evap}^{out} - T_{evap}^{in}) \quad (3.3)$$

$$\dot{Q}_{cond} = \dot{m}_{cond} \times C_p \times (T_{cond}^{in} - T_{cond}^{out}) \quad (3.4)$$

$$\dot{Q}_{cond} = \alpha_0 \times (\dot{Q}_{evap} + \dot{E}_{ch}) \quad (3.5)$$

The equations used for the chiller model required a certain level of abstraction before it could be utilized in the MILP. This could be achieved with the following four steps. The condenser-side of the chiller is similar to the evaporator-side, and hence it is not discussed.

- Substituting the COP with  $\dot{E}_{ch}$  using Eq. (3.2) and fixing  $T_{evap}^{in}$  and  $T_{cond}^{in}$  as GA variables (MILP parameters) in Eq. (3.1) results in  $\dot{E}_{ch}$  becoming a single-value function of  $\dot{Q}_{evap}$  (Eq. (3.6)).

$$\dot{E}_{ch} = \frac{\beta_0 T_{evap}^{in} + \beta_1 \frac{T_{cond}^{in} - T_{evap}^{in}}{T_{cond}^{in}} + \dot{Q}_{evap}}{\frac{T_{evap}^{in}}{T_{cond}^{in}} - \beta_2 \frac{\dot{Q}_{evap}}{T_{cond}^{in}}} - \dot{Q}_{evap} \quad (3.6)$$

- Piecewise linearization could then be applied, making  $\dot{E}_{ch}$  linearly dependent on  $\dot{Q}_{evap}$ . The linearized form is illustrated in Eqs. (3.7)–(3.9), where  $\alpha$ s are constants to be determined. Binary variables  $Y_i$ s were introduced to ensure that the appropriate linear section is used for the right range.

$$\dot{E}_{ch} = \sum_{i=1}^m \alpha_i \dot{Q}_{evap,i} + Y_i \alpha_2 \quad (3.7)$$

$$\dot{Q}_{evap,i}^{min} Y_i \leq \dot{Q}_{evap,i} \leq \dot{Q}_{evap,i}^{max} Y_i \quad \forall i \quad (3.8)$$

$$\sum_{i=1}^m Y_i \leq 1 \quad (3.9)$$

- $\dot{Q}_{evap}$  could be further decomposed using Eq. (3.3). Thus,  $\dot{E}_{ch} = f(\dot{m}_{evap}, T_{evap}^{out})$ . Employing the ‘reformulation-linearization-technique’ (RLT) further enabled the linearization of the product of  $\dot{m}_{evap}$  and  $T_{evap}^{out}$ , through the introduction of auxillary variables [35].

<sup>1</sup> Limitations of the raw data was the main reason the GNU model was selected over newer and better performing models [33,34].

**Table 2.2**

A general unit description.

Input variables	Description
$x_1$	First variable
$x_2$	Second variable
<b>Contribution to objective function</b>	
$y = \alpha_0 x_1 + \alpha_1 x_2 + \alpha_2 x_1 x_2 + \alpha_3$	$y$ represents the contribution to the objective function (electricity). The objective function is the summation of contribution from all units
<b>Capacity constraints</b>	
$F_{x_1}^{\min} Y_{x_1} \leq x_1 \leq F_{x_1}^{\max} Y_{x_1}$	$F^{\min/\max}$ represent the limits on the unit/variable. Using a chiller as an example, the limits could be used to represent its cooling capacity, flowrate etc. Binary variables ( $Y$ ) were introduced to turn the unit on and off
$F_{x_2}^{\min} Y_{x_2} \leq x_2 \leq F_{x_2}^{\max} Y_{x_2}$	
$Y_{x_1} + Y_{x_2} - 2Y = 0$	
<b>Streams</b>	
$z_i = \gamma_{0,i} x_1 + \gamma_{1,i} x_2 + \gamma_{2,i} x_1 x_2 + \gamma_{3,i}$	Streams represent inflow and outflows of material (fluid, energy, temperature etc.). These streams were used to interact with other units. A positive value of $z$ represented an inflow and vice versa. There could be as many streams ( $n = \sum i$ ) defined as required

### 3.2. Pump and network

Problem formulations in the literature reviewed were highly simplified, neglecting the pressure and temperature considerations in networks. To incorporate such considerations, the network models used in this section were formulated using analytical equations [36]. These factors were essential for addressing operation related problems.

Chilled(evaporator side)/warm(condenser side) water produced by chillers are transported via the piping network. The pump(s) and (piping) network were modeled collectively due to their high level of dependence. Two models were developed to capture the essence of the commonly used ‘primary-secondary’ pumping scheme [37], which was critical to determining the causes of inefficiencies in the system [38]. These models were designed to output the electricity consumed by pumps and the fluid return temperature while respecting physical and thermodynamic principles/constraints. The developed models describe the evaporator, condenser and distribution networks as shown in Fig. 1.1. Evaporator and condenser networks are similar and could be represented by the same model. The secondary network, however, was not included as it is usually out of the DCS operators’ jurisdiction.

#### 3.2.1. Key aspects of the pump and network model

Four aspects were identified to describe the network models comprehensively. The abstraction procedure is also discussed. For simplicity, thermal losses in the network were neglected.

##### • Pump electricity consumption for a given network

Pressure-flowrate curves of the pump and network were used for determining the operating point of the pump. The pressure-flowrate relationship for the pipelines in series was aggregated and represented by Eq. (3.10). With the assumption that the pump curves provided by the manufacturer were accurate, the coefficient  $\alpha$  was calibrated using raw data. Plots of electricity consumption versus flowrate of pumps at nominal speeds were used to determine the electricity consumed by the pump at the given operating point. To account for efficiency variation associated with varying rotational speed, the formula recommended by Marchi et al. was used [39].

$$\Delta P_{\text{sys}} = \alpha \dot{m}_{\text{sys}}^{1.852} \quad (3.10)$$

For pumps equipped with variable speed drives (VSD) and network with valves, the area enclosed by the pump curve at nominal speed, network curve when all valves are fully open, and the ordinate represents all possible operating points of a given configuration. Multi-variate linear regression was used to map the possible operating points of the pump-system configuration to its corresponding electricity consumption (Eq. (3.11)). The associated  $R^2$  values were always greater than 0.98 for the training datasets used.

$$\dot{E}_{\text{p,operating}} = \beta_0 \Delta P_{\text{sys}} + \beta_1 \dot{m}_{\text{sys}} + \beta_2 \quad (3.11)$$

The pressure-flowrate curves of the pump at maximum speed and system at lowest flow impedance (all valves fully open) were piecwise linearized and introduced as upper and lower bounds to the  $\Delta P_{\text{sys}}$  variable for accurate representation.

##### • Pressure-flowrate relationship in parallel networks

Majority of the DCS employ parallel network connections to the various customers. This configuration requires the pressure difference in each branch in the parallel assembly to be identical. Each parallel branch in the configuration is usually representative of a customer - a heat exchanger regulated by a valve. The following set of inequalities were introduced as constraints to the MILP formulation, such that the electricity consumed by the pump serving a parallel network could be determined.

$$\begin{aligned} \Delta P_{//,\text{sys}} &\geq \Delta P_{br,1} \\ \Delta P_{//,\text{sys}} &\geq \Delta P_{br,2} \\ &\vdots \\ \Delta P_{//,\text{sys}} &\geq \Delta P_{br,n} \end{aligned} \quad (3.12)$$

The variables to be optimized in the parallel network are the flowrates in each parallel branch.  $\Delta P_{br,i}$  was calculated using a given flowrate and the system curve at the lowest flowrate impedance. The set of inequalities and the placement of  $\Delta P_{//,\text{sys}}$  in the objective

**Table 2.3**

Layers description.

Layer type	Example equation	Description
Temperature	$T_1^{out} + \dots + T_n^{out} \leq T_1^{in} + \dots + T_m^{in}$	For DCS, the lower the supply temperature from the cooling source (chillers, etc.), the greater the electricity expended. As such, any optimal solution will try to raise the outlet temperatures as much as possible
Fluid flowrate	$\dot{m}_1^{out} + \dots + \dot{m}_n^{out} \geq \dot{m}_1^{in} + \dots + \dot{m}_m^{in}$	Should greater fluid flow be supplied than required, more electricity would be expended by pumps and chillers leading to sub-optimal solutions
Pressure	$\Delta P_1^{out} + \dots + \Delta P_n^{out} \geq \Delta P_1^{in} + \dots + \Delta P_m^{in}$	It is sub-optimal for a pump to supply greater pressure than required

function (Eq. (3.11)) ensured that  $\Delta P_{\text{f},\text{sys}}$  will always be equivalent to the branch with the highest  $\Delta P_{\text{br},i}$ . Since valves were implicitly included in each of the parallel branches, the selected configuration of flowrates will always be achieved. This was so as the respective valves could elevate the pressure difference in the parallel branches to the required level, enabling the flowrate configuration selected.

- **Temperature mixing of streams**

When multiple fluid streams of different temperatures mix, it is important to determine the temperature of the resultant stream. Such a consideration enables the supply and return temperatures of the distribution network to be determined. Energy and continuity equations were used for this purpose [36].

$$\dot{m}_{\text{sys}} = \dot{m}_{\text{br},1} + \dot{m}_{\text{br},2} + \dots + \dot{m}_{\text{br},n} \quad (3.13)$$

$$T^{\text{out}} = \frac{\dot{m}_{\text{br},1} T_{\text{br},1}^{\text{out}} + \dot{m}_{\text{br},2} T_{\text{br},2}^{\text{out}} + \dots + \dot{m}_{\text{br},n} T_{\text{br},n}^{\text{out}}}{\dot{m}_{\text{sys}}} \quad (3.14)$$

$$T^{\text{out}} = \% \dot{m}_{\text{br},1} T_{\text{br},1}^{\text{out}} + \% \dot{m}_{\text{br},2} T_{\text{br},2}^{\text{out}} + \dots + \% \dot{m}_{\text{br},n} T_{\text{br},n}^{\text{out}} \quad (3.15)$$

Eq. (3.14) contains fractional and bilinear terms. Fixing  $\dot{m}_{\text{sys}}$  as a GA variable (MILP parameter) results in Eq. (3.15), where  $\% \dot{m}_{\text{br},i}$  is the fraction of  $\dot{m}_{\text{sys}}$  for a given stream. RLT is then used to linearize the bilinear terms.

- **Substation level**

When  $\dot{m}_{\text{sys}}$  is fixed, the temperature of the fluid leaving the substation (customer heat exchanger) for a given cooling demand could be determined by manipulating the SFEE as shown in Eq. (3.16). Thus, the return temperature of the distribution network could be calculated by summing the product of  $\% \dot{m}_{\text{ss},i}$  and  $T_{\text{ss},i}^{\text{out}}$  (Eq. (3.17)). RLT was invoked once again for the linearization of this equation.

$$T_{\text{ss},i}^{\text{out}} = \frac{\dot{Q}_{\text{demand},i}}{\% \dot{m}_{\text{ss},i} \dot{m}_{\text{sys}} C_p} + T_{\text{ss},i}^{\text{in}} \quad (3.16)$$

$$T_{\text{dist\_nwk}}^{\text{out}} = \sum_{i=1}^m \frac{\dot{Q}_{\text{demand},i}}{\dot{m}_{\text{sys}} C_p} + \% \dot{m}_{\text{ss},i} T_{\text{ss},i}^{\text{in}} \quad (3.17)$$

A constraint was imposed on the temperature difference ( $\Delta T_{\text{ss},i}$ ) and supply temperature ( $T_{\text{ss},i}^{\text{in}}$ ) on the ‘cold-side’ of the heat exchanger to compensate for the absence of a substation model. This was done so that the optimization results generated would be realistic and feasible. The constraints ensured that  $\Delta T_{\text{ss},i}$  and  $T_{\text{ss},i}^{\text{in}}$  did not exceed the nominal values specified.

$$\frac{\% \dot{m}_{\text{ss},i} \dot{m}_{\text{sys}} C_p}{\dot{Q}_{\text{demand},i}} \geq \frac{1}{\Delta T_{\text{limit,ss},i}} \quad (3.18)$$

$$T_{\text{ss},i}^{\text{in}} \leq T_{\text{limit,ss},i}^{\text{in}} \quad (3.19)$$

### 3.2.2. Evaporator network model

The purpose of this model is to calculate the electricity consumption of the pumps and the supply temperature of chilled water to the evaporator network. Chillers could supply chilled water at various temperatures. The following steps detail the assembly of the evaporator network model. The same procedure was used to implement the condenser network.

- By fixing  $\dot{m}_{\text{sys}}$  as a GA variable (MILP parameter), the supply temperature to the distribution network could be expressed linearly by using RLT on Eq. (3.15).

- To determine the electricity for a given flowrate, Eq. (3.10) was linearized before being used as input to Eq. (3.11).
- Finally, to ensure that the operating pressures of the pump do not exceed the lower and upper bounds imposed by the pump and system curves, the curves were piecewise linearized and imposed as constraints.

### 3.2.3. Distribution network model

The purpose of this model is to calculate the electricity consumption of the pumps and determine the supply temperature of water returning to the chillers. The procedure is similar to the evaporator network model except for the following differences.

- Eq. (3.12) was used to calculate the pressure drop in the parallel network before being used as input to Eq. (3.11).
- For a given set of demands ( $\dot{Q}_{\text{demand},i}$ ), RLT was applied to Eq. (3.17), so that it could be expressed linearly.

### 3.2.4. Cooling tower

Cooling towers are often used for heat rejection in a typical DCS (Fig. 1.1). They represent the most economical mode of rejecting heat in the absence of natural options (sea, lake). The objective of this model is to use flowrate and temperature to predict the range of the cooling tower and the corresponding electricity consumed.

The universal engineering model (UEM) for cooling towers was selected despite the existence of models which are potentially more accurate [40–42]. The lack of differential equations made it easier to linearize. Second order Taylor's series expansion enabled the heat transfer effectiveness function to be expressed as a quadratic equation. The resulting empirical model illustrated good performance when compared to the often used Braun's model. The describing equation for the model is as follows.

$$\begin{aligned} \varepsilon = & \beta_0 + \beta_1 \left[ \frac{\dot{m}_{\text{air}}^{\text{in}}}{\dot{m}_{\text{ct}}^{\text{in}}} \right] + \beta_2 [T_{\text{ct}}^{\text{in}} - T_{\text{wb}}] + \beta_3 \left[ \frac{\dot{m}_{\text{air}}^{\text{in}}}{\dot{m}_{\text{ct}}^{\text{in}}} \right]^2 + \beta_4 [T_{\text{ct}}^{\text{in}} - T_{\text{wb}}]^2 \\ & + \beta_5 \left[ \frac{\dot{m}_{\text{air}}^{\text{in}}}{\dot{m}_{\text{ct}}^{\text{in}}} \right] [T_{\text{ct}}^{\text{in}} - T_{\text{wb}}] \end{aligned} \quad (3.20)$$

where  $\varepsilon$  is,

$$\varepsilon = \frac{\dot{m}_{\text{ct}}^{\text{in}} C_p T_{\text{ct}}^{\text{in}} + \dot{m}_{\text{mu}}^{\text{in}} C_p T_{\text{mu}}^{\text{in}} - \dot{m}_{\text{ct}}^{\text{out}} C_p T_{\text{ct}}^{\text{out}}}{\dot{m}_{\text{ct}}^{\text{out}} C_p (T_{\text{ct}}^{\text{in}} - T_{\text{wb}})} \quad (3.21)$$

Finally, the component which consumes electricity in the cooling tower unit is the fan. A linear relationship between the flowrate and electricity consumed was assumed. The impact of this assumption on the final objective is small as cooling towers tend to represent a small percentage of electricity consumption of DCS.

$$\dot{E}_{\text{ct}} = \gamma \dot{m}_{\text{ct}}^{\text{in}} \quad (3.22)$$

Cooling tower models are often complex as they involve heat and mass transfer equations. The following measures were taken to simplify the equations listed above. Since the value of make-up water is usually very small, it is difficult to get high quality data on its flowrate and temperature. Thus, the assumption that  $\dot{m}_{\text{ct}}^{\text{in}} \approx \dot{m}_{\text{ct}}^{\text{out}}$  led to the simplification of Eq. (3.21), yielding Eq. (3.23).

$$\begin{aligned} \frac{T_{\text{ct}}^{\text{in}} - T_{\text{ct}}^{\text{out}}}{T_{\text{ct}}^{\text{in}} - T_{\text{wb}}} = & \beta_0 + \beta_1 \left[ \frac{\dot{m}_{\text{air}}^{\text{in}}}{\dot{m}_{\text{ct}}^{\text{in}}} \right] + \beta_2 [T_{\text{ct}}^{\text{in}} - T_{\text{wb}}] + \beta_3 \left[ \frac{\dot{m}_{\text{air}}^{\text{in}}}{\dot{m}_{\text{ct}}^{\text{in}}} \right]^2 \\ & + \beta_4 [T_{\text{ct}}^{\text{in}} - T_{\text{wb}}]^2 + \beta_5 \left[ \frac{\dot{m}_{\text{air}}^{\text{in}}}{\dot{m}_{\text{ct}}^{\text{in}}} \right] [T_{\text{ct}}^{\text{in}} - T_{\text{wb}}]. \end{aligned} \quad (3.23)$$

Since the total flowrate in the condenser network had to treated as a GA variable (MILP parameter), this meant that the flowrate through each tower is also fixed. The same is true for  $T_{\text{ct}}^{\text{out}} = T_{\text{ch},i}^{\text{in}}$ . Thus Eq. (3.23) could be simplified into Eq. (3.24) using regression. RLT was then applied for complete linearization.

$$\Delta T_{ct} = \nu_0 T_{ct}^{in} + \nu_1 \dot{m}_{air}^{in} + \nu_2 T_{ct}^{in} \dot{m}_{air}^{in} + \nu_3 \quad (3.24)$$

where  $\Delta T_{ct} = T_{ct}^{in} - T_{ct}^{out}$ .

#### **4. Case study: problem formulation**

#### *4.1. Description*

The case study discussed in this section is based on a functioning DCS located in Europe. The expected performance of a DCS is usually entirely different from reality owing to the limited information available during the design phase. Various factors could have contributed to the degraded performance of DCS; the lack of cooling demand and less than ideal system design are two common reasons for this occurrence. Development at the site of the DCS was slower than projected due to economic reasons. Without sufficient demand, the DCS cannot operate as efficiently as intended. Therefore, the purpose of this case study is to identify possible changes in operating practices which could potentially improve energy efficiency. The hierarchical optimization framework is employed for the undertaking.

The DCS of interest comprised of a single central station serving four customers of different load profiles (commercial, retail, office). The central station houses three water-cooled chillers - one small and two large ones, cooled by an array of 5 cooling towers (Fig. 4.1).

Current operating practices, coupled with low demand, often resulted in the infamous ‘low  $\Delta T$ ’ syndrome’, where the pumps operate at

near maximum capacity while chillers operate inefficiently at low part-load conditions. The purpose of this study is to investigate the extent to which operating practices can be tuned to improve energy usage. This is not a trivial task as it involves the adjustment of many dependent variables with unclear implications, resulting in the need for optimization to be done.

The objective is to optimize the operation of DCS at the hourly level using the framework discussed in Section 2. Models discussed in Section 3 are used to detail the DCS to the component level before the application of the optimization strategy. Demand conditions for three representative days with low, medium and high cooling demands were selected to illustrate the benefits of performing optimization on the system.

The input conditions such as the cooling demand profile and the ambient conditions are shown in Figs. 4.2 and 4.3 respectively.

#### 4.2. Implementation of optimization framework

**Table 4.1** describes the variables and parameters involved at each time-step. The variables are separated into master and slave level variables. These variables are handled separately in different phases of the optimization framework. Optimization of electricity over a 24 h period involved 684 variables. The problem was simplified using the assumption that every time-step, comprising a 1-h duration, is independent. The overall ‘optimal’ value, therefore, is the summation of ‘optimal’ values of each time-step.

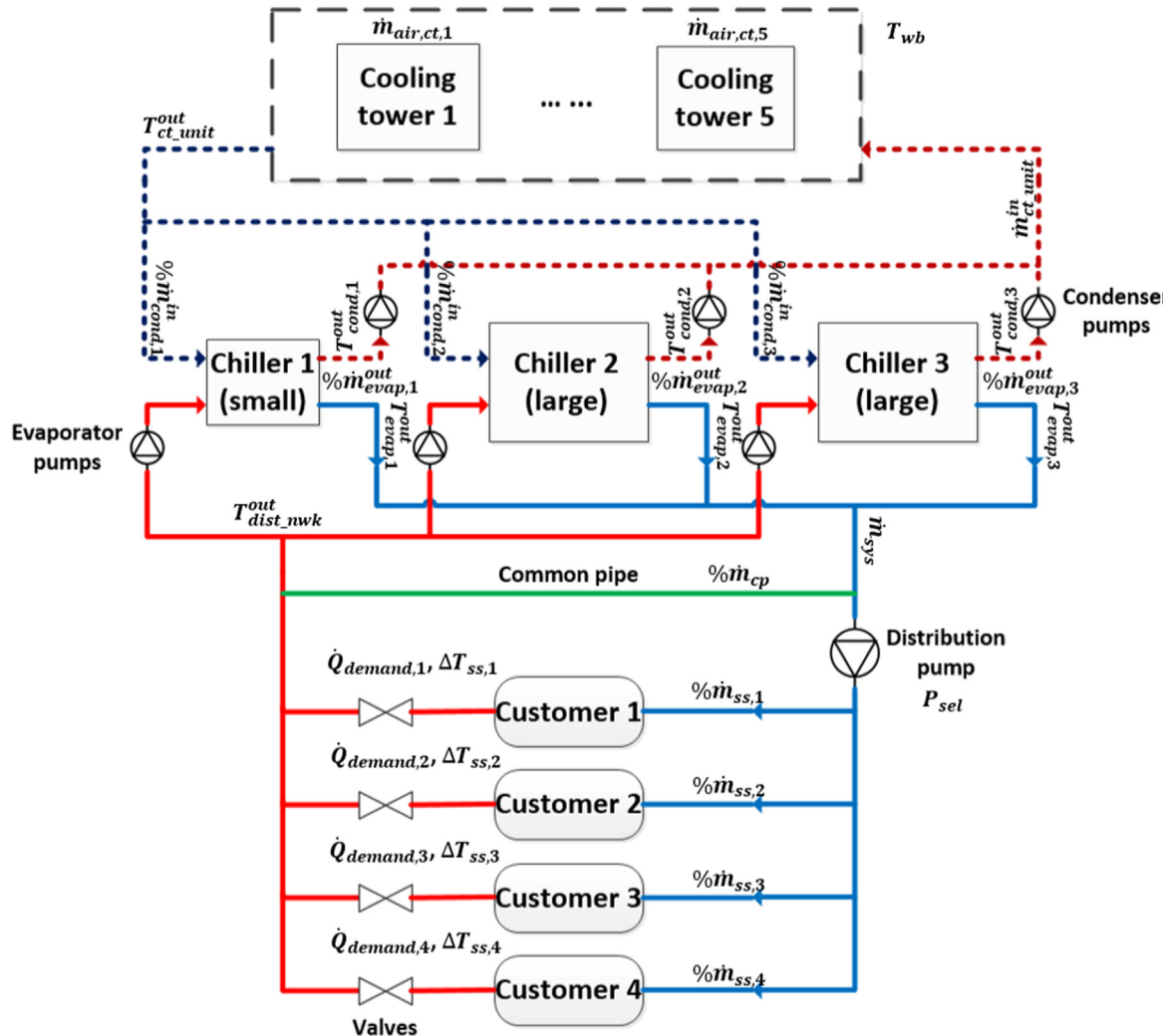


**Fig. 4.1.** Schematic of DCS in case study

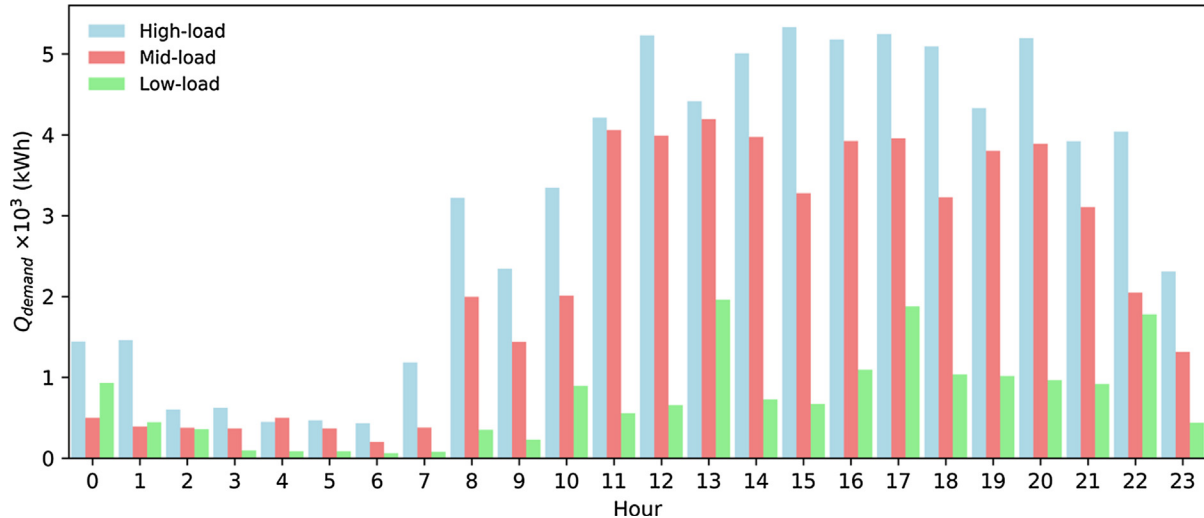


Fig. 4.2. Customer demand profiles of the three chosen periods.

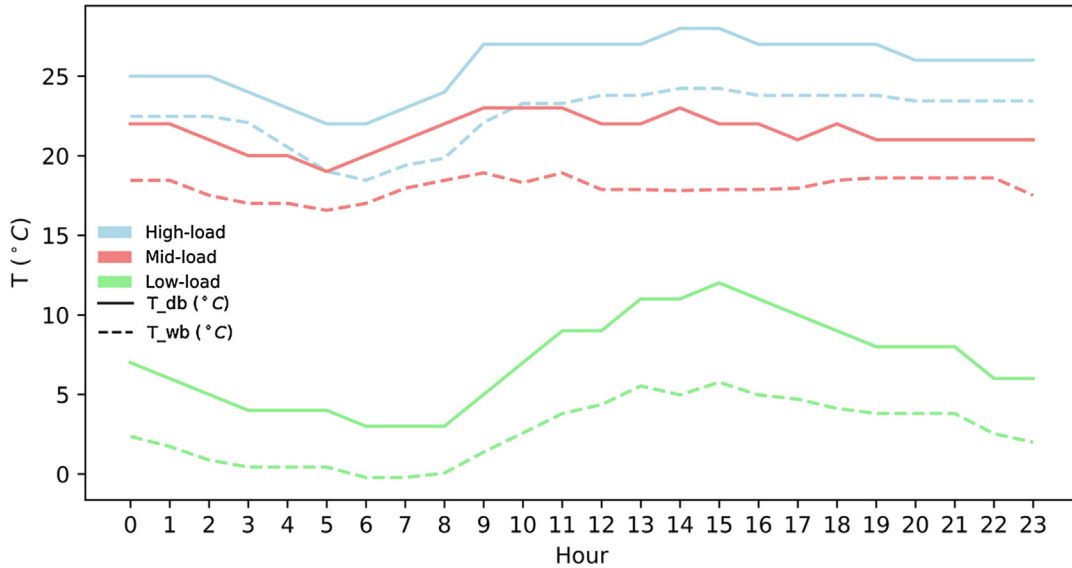


Fig. 4.3. Ambient condition profiles of the three chosen periods.

#### 4.2.1. Mathematical formulation

This section illustrates the mathematical formulation of the decomposition approach. The objective function is defined as the minimization of hourly electricity consumption of the DCS.

**4.2.1.1. Master level.** The overall objective function for each hour is defined as:

$$\text{minimize } \dot{E}_{\text{DCS}} = f(T_{\text{ct-unit}}^{\text{out}}, \dot{m}_{\text{ct-unit}}^{\text{in}}, T_{\text{dist-nwk}}^{\text{out}}, \dot{m}_{\text{sys}}) \quad (4.1)$$

Variables at the master level are treated as parameters at the slave level and used for the computation of various coefficients which ensures that the slave is a MILP. For each set of master level variables, the slave returns an optimal solution. The process is iterated until a convergence criteria is met.

**4.2.1.2. Slave level.** The objective function at the slave level is:

$$\begin{aligned} \text{minimize } \dot{E}_{\text{slave}} = & \sum_{i=1}^{n=3} \dot{E}_{\text{ch},i} + \sum_{i=1}^{n=3} \dot{E}_{\text{evap-nwk},p,i} + \sum_{i=1}^{n=3} \dot{E}_{\text{cond-nwk},p,i} \\ & + \sum_{i=1}^{n=7} \dot{E}_{\text{dist-nwk},p,i} + \sum_{i=1}^{n=5} \dot{E}_{\text{ct},i} \end{aligned} \quad (4.2)$$

With  $T_{\text{ct-unit}}^{\text{out}}$ ,  $\dot{m}_{\text{ct-unit}}^{\text{in}}$ ,  $T_{\text{dist-nwk}}^{\text{out}}$  and  $\dot{m}_{\text{sys}}$  treated as parameters, the electricity consumed by the chiller and the associated constraints are defined as:

$$\dot{E}_{\text{ch},i} = f(\% \dot{m}_{\text{evap},i}^{\text{out}}, T_{\text{evap},i}^{\text{out}}, \% \dot{m}_{\text{cond},i}^{\text{in}}) \quad (4.3)$$

The flowrate percentages and temperatures are required for the calculation electricity consumption of the chiller.

With the total network flowrates ( $\dot{m}_{\text{ct-unit}}^{\text{in}}$  and  $\dot{m}_{\text{sys}}$ ) fixed as parameters, the electricity consumed by the evaporator and condenser pumps could be expressed as follows.

$$\dot{E}_{\text{evap-nwk},p,i} = f(\% \dot{m}_{\text{evap},i}^{\text{out}}) \quad (4.4)$$

$$\dot{E}_{\text{cond-nwk},p,i} = f(\% \dot{m}_{\text{cond},i}^{\text{in}}) \quad (4.5)$$

The following equations are involved in the computation of the electricity consumed by the distribution pump given that  $\dot{m}_{\text{sys}}$  is a parameter.

$$\sum_{i=1}^{n=7} \dot{E}_{\text{dist-nwk},p,i} = Y_{\text{dist-nwk},p,i} f(\% \dot{m}_{\text{ss},1}, \dots, \% \dot{m}_{\text{ss},4}) \quad (4.6)$$

**Table 4.1**

Parameters and variables associated with the case study.

Master level variables	Description
$T_{ct\_unit}^{out}$ (K)	temperature of fluid exiting the cooling tower array and entering the condenser side of chillers
$\dot{m}_{ct\_unit}^{in}$ (kg/s)	total condenser network flowrate
$T_{dist\_nwk}^{out}$ (K)	temperature of return fluid from the distribution network entering the evaporator side of chillers.
$\dot{m}_{sys}$ (kg/s)	total evaporator/distribution network flowrate
<b>Slave level variables</b>	
$\% \dot{m}_{evap,i}^{out}$	percentage of total flowrate through the $i$ th chiller evaporator.
$T_{evap,i}^{out}$ (K)	fluid temperature exiting $i$ th chiller evaporator.
$T_{cond,i}^{out}$ (K)	fluid temperature exiting $i$ th chiller condenser.
$\% \dot{m}_{cond,i}^{in}$	percentage of total flowrate through the $i$ th chiller condenser
$\% \dot{m}_{cp}$	percentage of total flowrate through the common pipe.
$\% \dot{m}_{ss,i}$	percentage of total flowrate through the $i$ th customer's substation.
$\dot{m}_{air,ct,i}$ (kg/s)	induced air flowrate through each cooling tower
$P_{sel}$	the choice/combinations of distribution pump(s)
<b>Parameters</b>	
$\dot{Q}_{demand,i}$ (kWh)	cooling demand of the $i$ th customer substation.
$T_{wb}$ (K)	thermodynamic wet-bulb temperature
$\Delta T_{max,ss,i}$ (K)	maximum temperature difference on the cold-side of the heat-exchanger at the substation

$$\sum_{i=1}^{n=7} Y_{dist\_nwk,p,i} \leq 1 \quad (4.7)$$

Eq. (4.6) captures the impact of flowrate distribution in the parallel network on pressure difference and hence the electricity consumed by the distribution pump. Eq. (4.7) ensures that only one pump or pump

**Table 4.2**

Decision variable settings of the DCS in the 3 optimization cases defined.

		'Base-case'	'Chiller optimization'	'Holistically optimized'
Decision variables	$\Delta T_{approach}$ (K)	Fixed	Fixed	Variable
	$\dot{m}_{cond,i}$ (kg/s)	Fixed	Fixed	Variable
	$\dot{m}_{evap,i}$ (kg/s)	Fixed	Variable	Variable
	$T_{evap,i}^{out}$ (K)	Fixed	Variable	Variable
	$\Delta T_{ss,i}$	Averaged from raw data.	Variable	Variable
	$P_{sel}$	Staged based on flowrates	Variable	Variable
	$Y_{ch,i}$	Staged based on flowrates	Variable	Variable

combinations are selected for serving the distribution network. The selected pump is described by the variable  $P_{sel}$ .

Given  $T_{ct\_unit}^{out}$ ,  $\dot{m}_{ct\_unit}^{in}$  and  $T_{wb}$  as parameters, the electricity consumed by the cooling tower is,

$$\dot{E}_{ct,i} = f(\% \dot{m}_{cond,1}^{in}, T_{cond,1}^{out}, \dots, \% \dot{m}_{cond,3}^{in}, T_{cond,3}^{out}, \dot{m}_{air,ct,i}) \quad (4.8)$$

where  $T_{cond,i}^{out}$  is an output of the chiller model.

An heat-exchanger model was excluded due to the lack of control over the 'hot-side' of the substation as described in Section 3.2.1. The temperature difference at each substation is,

$$\Delta T_{ss,i} = \frac{\dot{Q}_{demand,i}}{\dot{m}_{ss,i} \dot{m}_{sys} C_p} \quad (4.9)$$

$$\Delta T_{ss,i} \leq \Delta T_{max,ss,i} \quad (4.10)$$

Several additional constraints were needed to model the dependence between the equipment in the DCS. These are captured using the

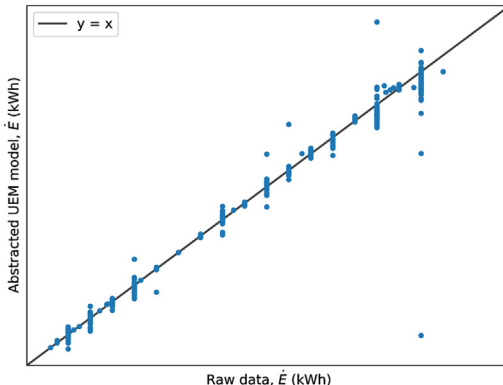
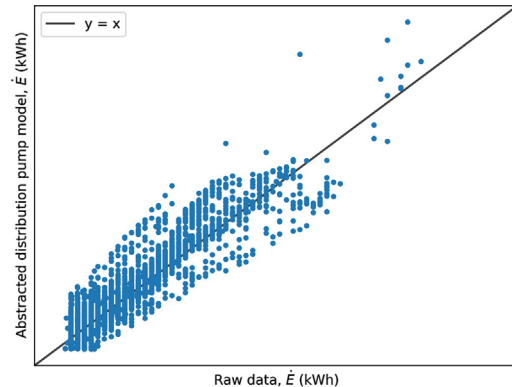
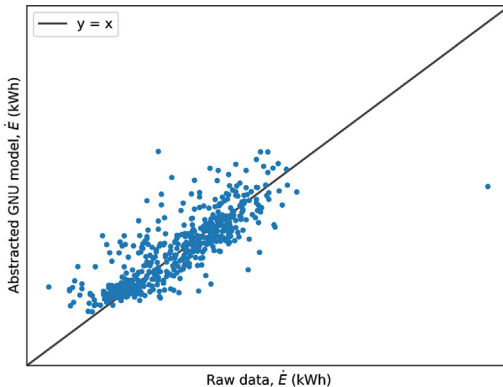
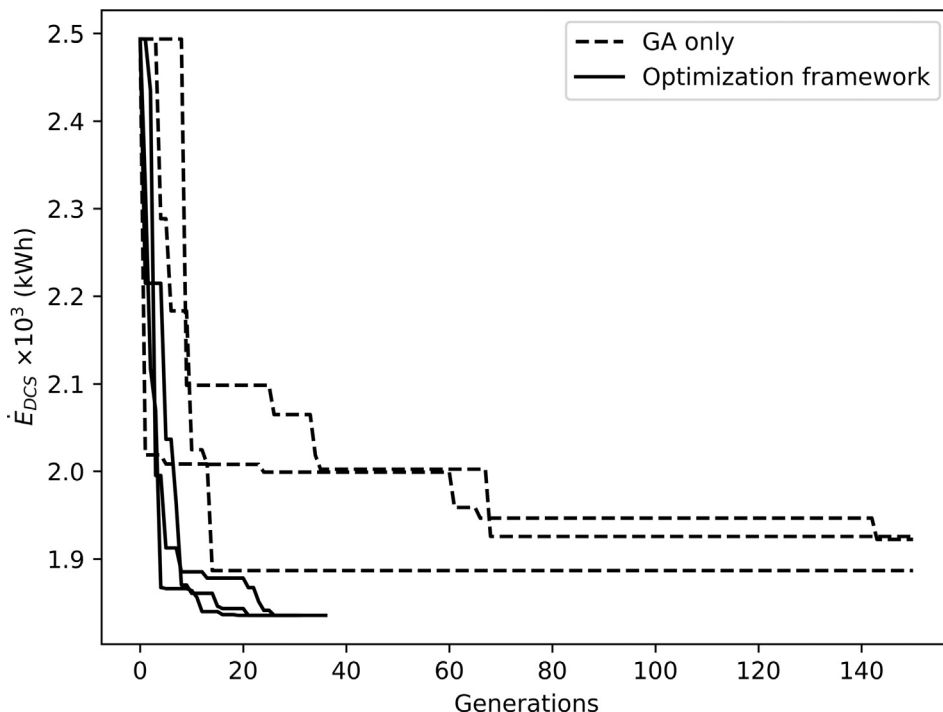


Fig. 4.4. Error plots of the chosen models used in the case-study.



**Fig. 5.1.** Performance comparison between the direct application of GA and the optimization framework.

**Table 5.1**  
GA hyperparameters for both approaches.

	GA only	Optimization framework
Number of GA variables	4	22
Population size	100	550
Tournament size	30	165
Crossover percentage	0.4	0.4
Mutation percentage	0.1	0.1

layer definition (Section 2.3.2). The flowrates in the DCS could be described by,

$$\sum_{i=1}^{n=3} \% \dot{m}_{evap,i}^{out} \geq \left[ \% \dot{m}_{cp} + \sum_{i=1}^{n=4} \% \dot{m}_{ss,i} \right] \geq 1 \quad (4.11)$$

$$\sum_{i=1}^{n=3} \% \dot{m}_{cond,i}^{in} \geq 1 \quad (4.12)$$

The temperatures in the DCS could be described by:

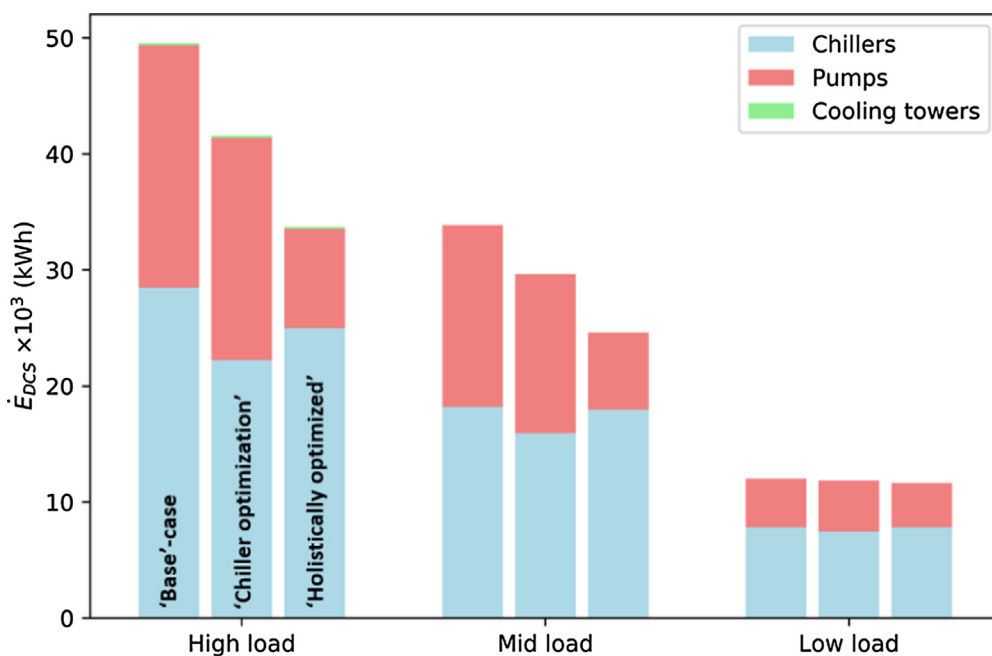


**Fig. 5.2.** Result comparison of the three optimization cases over the three representative periods.

**Table 5.2**

Percentage change in electricity consumption across the representative periods.

	'base' vs 'chiller optimization'	'base' vs 'holistically optimized'	'chiller optimization' vs 'holistically optimized'
<b>High load</b>			
Chillers	-21.94	-12.28	12.36
Pumps	-8.24	-58.95	-55.26
Cooling towers	0.00	-5.00	-5.00
Overall	-16.07	-31.93	-18.89
<b>Mid load</b>			
Chillers	-12.45	-1.36	12.66
Pumps	-12.58	-57.56	-51.45
Cooling towers	0.00	0.00	0.00
Overall	-12.51	-27.38	-17.00
<b>Low load</b>			
Chillers	-4.81	0.06	5.12
Pumps	5.33	-8.81	-13.42
Cooling towers	0.00	0.00	0.00
Overall	-1.28	-3.03	-1.77

**Table 5.3**

Working hours of chillers in DCS.

Working hours (h)					
		Chiller 1	Chiller 2	Chiller 3	Total
High-load	'Base'- case	14	18	7	39
	'Holistically optimized'	7	8	11	26
Mid-load	'Base'- case	17	15	0	32
	'Holistically optimized'	12	6	8	26
Low-load	'Base'- case	18	9	0	27
	'Holistically optimized'	16	7	2	25

$$\sum_{i=1}^{n=4} T_{\text{evap\_nwk}}^{\text{out}} + \Delta T_{\text{ss},i} \leq T_{\text{dist\_nwk}}^{\text{out}} \quad (4.13)$$

$$\sum_{i=1}^{n=5} T_{\text{cond\_nwk}}^{\text{out}} + \Delta T_{\text{ct},i} \leq T_{\text{ct\_unit}}^{\text{out}} \quad (4.14)$$

where  $T_{\text{evap\_nwk}}^{\text{out}}$ ,  $T_{\text{cond\_nwk}}^{\text{out}}$  and  $\Delta T_{\text{ct},i}$  could be calculated using the following equations,

$$T_{\text{evap\_nwk}}^{\text{out}} = f(\dot{m}_{\text{evap},1}^{\text{out}}, T_{\text{evap},1}^{\text{out}}, \dots, \dot{m}_{\text{evap},3}^{\text{out}}, T_{\text{evap},3}^{\text{out}}) \quad (4.15)$$

$$T_{\text{cond\_nwk}}^{\text{out}} = f(\dot{m}_{\text{cond},1}^{\text{in}}, T_{\text{cond},1}^{\text{out}}, \dots, \dot{m}_{\text{cond},3}^{\text{in}}, T_{\text{cond},3}^{\text{out}}) \quad (4.16)$$

$$\Delta T_{\text{ct},i} = f(\dot{m}_{\text{ct\_unit}}^{\text{in}}, \dot{m}_{\text{air,ct},i}^{\text{out}}, T_{\text{cond\_nwk}}^{\text{out}}) \quad (4.17)$$

The linearization process of the original models was described in Section 3. After the linearization process, the equations are structured in the form described in Section 2.3.

#### 4.2.2. Modeling error

75% and 25% of the processed data were used for training and the evaluation of the models respectively (Fig. 4.4). The mean absolute error for the models representing the chiller, distribution pumps and cooling towers are 11.3%, 6.9%, and 1.8% respectively. The evaporator and condenser pumps report similar values to the distribution pumps. The aggregation of data over hourly time-horizon coupled with inaccuracies in the sensor readings were likely causes to the noise in the data. Nevertheless, the models can capture the performance of the equipment as evidenced by the plots.

#### 4.2.3. Definition of a base-cases

Simulation of the current operating practices using the chosen

models is used as a benchmark for the evaluation of the results derived from the optimization strategy. These operating practices were a mixture of commonly employed control strategies for chiller plants [13,14]. Results of the simulation are also used for 'seeding' the GA to eliminate any chance of the optimal value being worse-off than the 'base-case'.

Additionally, chiller-only optimization was also defined to highlight the benefits performing holistic optimization on the DCS. For this scenario, each chiller is permitted to optimize variables independent to the unit, while respecting the constraints of other units. Table 4.2 lists the treatment of key variables in the both cases.

All computations were done on a workstation with 16 GB of RAM, and an i7 4710HQ CPU clocked at 3.5 GHz on all cores. The cumulative time required for a single run of the model reduction to post-processing phases averaged at 40 s. Solving the slave sub-problem, however, only required approximately 5 s. For the GA, a population size of 100 was defined and evaluated until there is no change in objective function for 10 generations. For the MILP, the solver was set to terminate should the optimality gap between the lower and upper objective bound is below  $10^{-4}$ .

## 5. Results and discussion

### 5.1. Comparison of approaches: GA only and the optimization framework

The advantage of using the optimization framework over the direct application of the GA onto the case study is highlighted in Fig. 5.1. Both methods were used to optimize the electricity consumption for a given demand for a single hour. Hyperparameter settings for the GAs used in both approaches are detailed in Table 5.1. The six trials were allowed to iterate for the same time duration.

Without the need to execute of MILP solvers, the GA only approach could complete evaluating more generations than the optimization framework. However, the value of the final objective function from the GA only approach left much to be desired - despite iterating through more generations; they did not deliver the same objective function value for the each of the three trials. The result is intuitive for the decomposition approach as the reduced number of variables to be optimized by the GA, allowed it to converge to a superior solution more quickly.

### 5.2. Case study results

The cumulative electricity consumptions of the DCS for the 'base', 'chiller optimization' and 'holistically optimized' cases are plotted in Fig. 5.2. A decrease in electricity consumption of 31.93%, 27.38%, and 3.03% was observed across the three 24 h periods representing high, medium and low cooling demand respectively between the first and third cases. Table 5.2 details the breakdown of the decrease in electricity consumption by component.

For data confidentiality, all numbers were scaled by a common factor. The order of magnitude is still preserved.

Not all components experienced the same rate of decrease in electricity consumption despite the overall figures. That highlights the benefit of performing optimization holistically as compared to the chiller-only approach, as the results are not apparent. Overall, the savings in the operation of the pumps are the most significant contributors to the savings in electricity. Optimization of the chillers, independent of the pump operations neglected this opportunity for added electricity savings. This effect is clearly illustrated when comparing the results of the chiller-only and the holistic approach. At the 'optimum' chillers were operated up to 12% less efficient in the holistic as compared to the chiller-only optimization approach. The slight reduction in chiller efficiencies, enabled the pumps to be operated more efficiently, thereby contributing to greater electricity savings for the entire system. The concurrent changes in chiller and network operation are the main reasons for this occurrence. The following discussions explain the

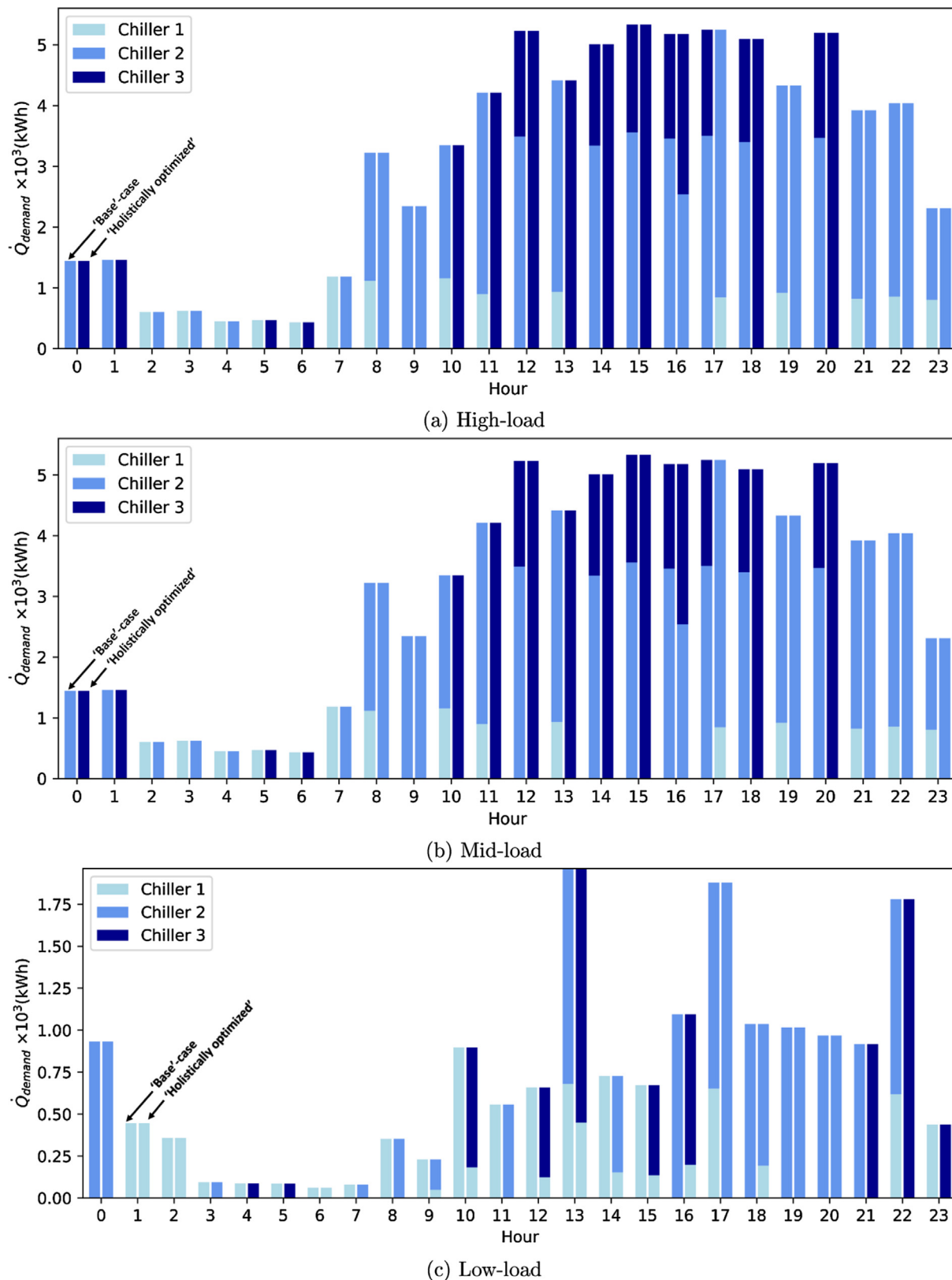
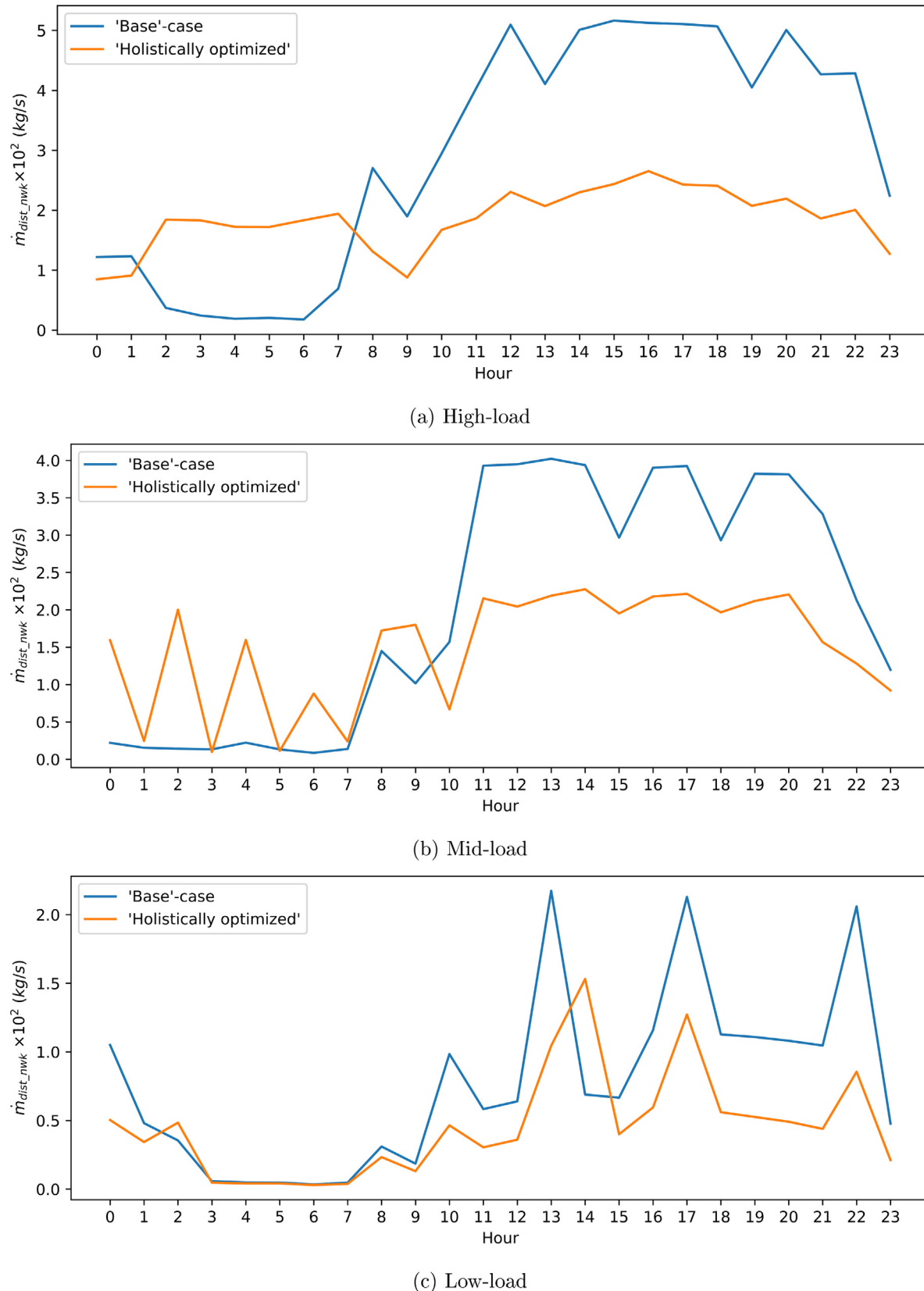


Fig. 5.3. Comparison of chiller staging strategies between the 'base' and 'holistically optimized' cases.

reasons for the electricity savings from the perspective of the chiller and distribution network operation by comparing the results of holistic optimization against the 'base' case. The discussion omits the impact of the cooling towers as they were hardly in operation due to the relatively low ambient temperatures (Fig. 4.3).

As there exists a minimum flowrate on the evaporator side of every chiller, more chillers in operation generally implied an increase in chilled water flowrate which loaded the pumps more heavily. The cumulative operating hours of the 'holistically optimized' cases are always lower than their corresponding 'base' cases (Table 5.3). This meant that



**Fig. 5.4.** Comparison of  $\dot{m}_{dist\_nwk}$  in the distribution network between the 'base' and 'holistically optimized' cases.

fewer chillers are activated to meet the cooling demand which results in a reduced load on the pumps.

There could be several explanations for this occurrence. For illustration purposes, the chiller staging strategies and the flowrates in the

distribution network for all three load scenarios are plotted in Figs. 5.3 and 5.4. It can be seen that under the 'holistically optimized' operating strategy, there is a general preference for operating as few chillers as possible. For fewer activated chillers with lower flowrates to fulfill the

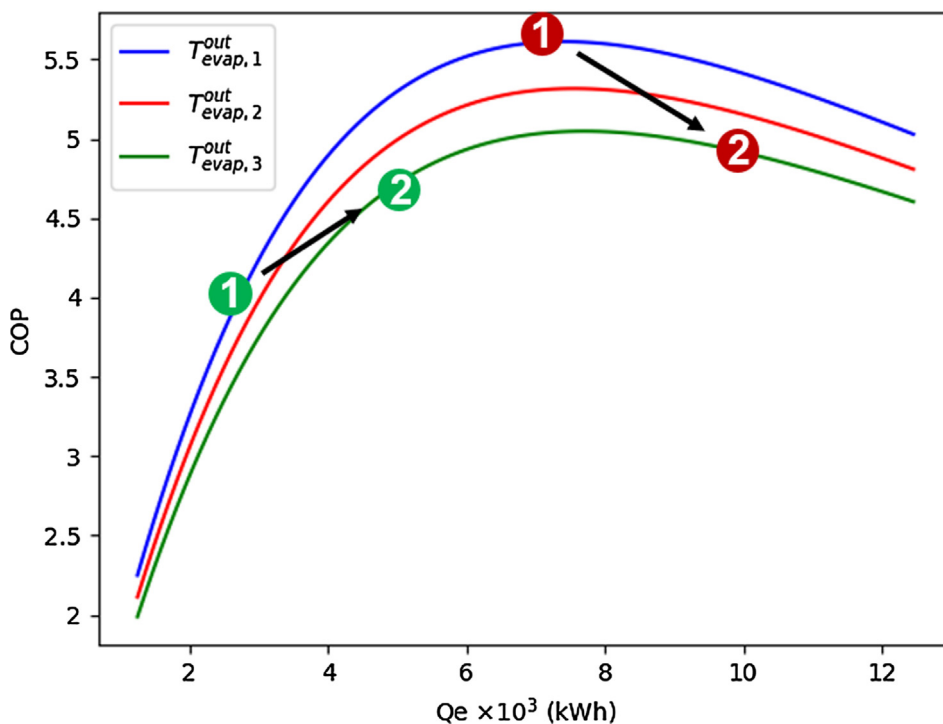


Fig. 5.5. Impact of lowering chilled water temperatures at various points of the part-load curve.

same cooling demand, the chilled water supply temperatures ( $T_{evap,i}^{out}$ ) of chillers had to be lowered. These lowered temperatures increased the thermal energy content of the working fluid which enabled the cooling demand to be met. The impact of such an action is usually unclear; lower chilled water supply temperature increases compressor lift which decreases energy efficiency. Conversely, general improvements in loading conditions had the opposite effect. This effect is illustrated in the part-load performance plot of one of the chillers in the case study (Fig. 5.5). Additional consideration of the impacts on pumps and networks further complicated the outcome.

Scenarios also exist whereby operating a larger chiller is more economical for the entire system. This could be seen from the period spanning from 0100hrs to 0700hrs across all three load scenarios (Fig. 5.3). Operating a larger chiller meant that the criteria for the minimum flowrate had to be raised (Fig. 5.4). Raising the flowrate negatively impacted the  $\Delta T$  of the distribution network. However, due to chiller 2 and 3 being dual-compressor systems, having a single compressor activated meant that it had the luxury of utilizing the entire heat-exchange surface area on both the condenser and evaporator sides. That results in a higher COP as compared to operating chiller 1 for the given load.

There are uncommon instances where (low-load, Table 5.2) where the ‘holistically optimized’ results suggest that chillers should operate less efficiently for the benefit of the overall system performance.

It is thus, worthwhile to investigate the operation of the distribution network since the pump operations at the ‘optimum’ are the largest contributors to the overall electricity savings. It has been established that the lower chilled water supply temperatures ( $T_{evap,i}^{out}$ ) reduces the overall flowrate and hence the load on the pumps. That, however, is only just one side of the equation. Comparison of Figs. 5.4 and 5.6 reveals a positive relationship between the flowrate ( $\dot{m}_{dist\_nwk}$ ) and the pressure difference ( $\Delta P_{dist\_nwk}$ ) in the distribution network. While that is generally true, the reduction of  $\Delta P_{dist\_nwk}$  could also be explained by another factor - valve regulation at the substation level of customers’.

Most of the above explanations is focused on how lowering chilled water supply temperatures, reduces the overall flowrate in the distribution network and hence the electricity consumption of the pumps.

Fig. 5.7 compares the temperature difference at the substation level ( $\Delta T_{ss,i}$ ) between the ‘base’ and ‘holistically optimized’ cases. A reduction of distribution network flowrate should increase the value of  $\Delta T_{ss,i}$  across the board, however, scenarios exist, at the ‘optimum’ where the value of  $\Delta T_{ss,i}$  is lower than that of the ‘base’ case. Intuitively, this should not happen as only serves to degrade the return temperature to the chillers ( $T_{dist\_nwk}^{out}$ ), which will adversely impact the efficiency of chillers. The reason for this observation becomes clearer only when analyzing the results from the standpoint of network pressure difference. In a parallel network configuration with each branch independently controlled by a valve, the situation with the lowest flow impedance occurs when all valves are fully open. Partially closing a valve in any branch will serve to impede flow and subsequently increase the pressure difference of the entire network. Depending on the cooling demand scenario, it is hence, conceivable that some valves regulated such that more chilled water flows through a given substation than required. Doing so, despite compromising on  $\Delta T_{dist\_nwk}$  saves electricity by reducing  $\Delta P_{dist\_nwk}$ . This effect is most commonly observed in the mid-load condition (Fig. 5.7b).

The benefits of applying optimization to the DCS were highlighted in the case study. Optimization of DCS at the system level extended beyond the consideration of chillers alone. This was especially true in DCS where considerable energy was used in the distribution of chilled water. There were even instances where a slight reduction of chiller efficiencies resulted in overall electricity savings at the system level. Reduction of chilled water supply temperatures to prevent another chiller from being activated was one such example. For a system with such tight-coupling between components, the best operating strategy is usually non-trivial.

There were limitations to the extent of improvement, however. At extremely low loads, little could be done to improve the operation of the DCS. This was a design level issue which had to be dealt with separately. The proposed methods of improving system performance could be used as short-term measures, as well as a guide for further improvements in design. For instance, it may not be ideal to supply chilled water colder than required for prolonged periods. Should the operation of DCS at part-load conditions be expected to prevail, perhaps

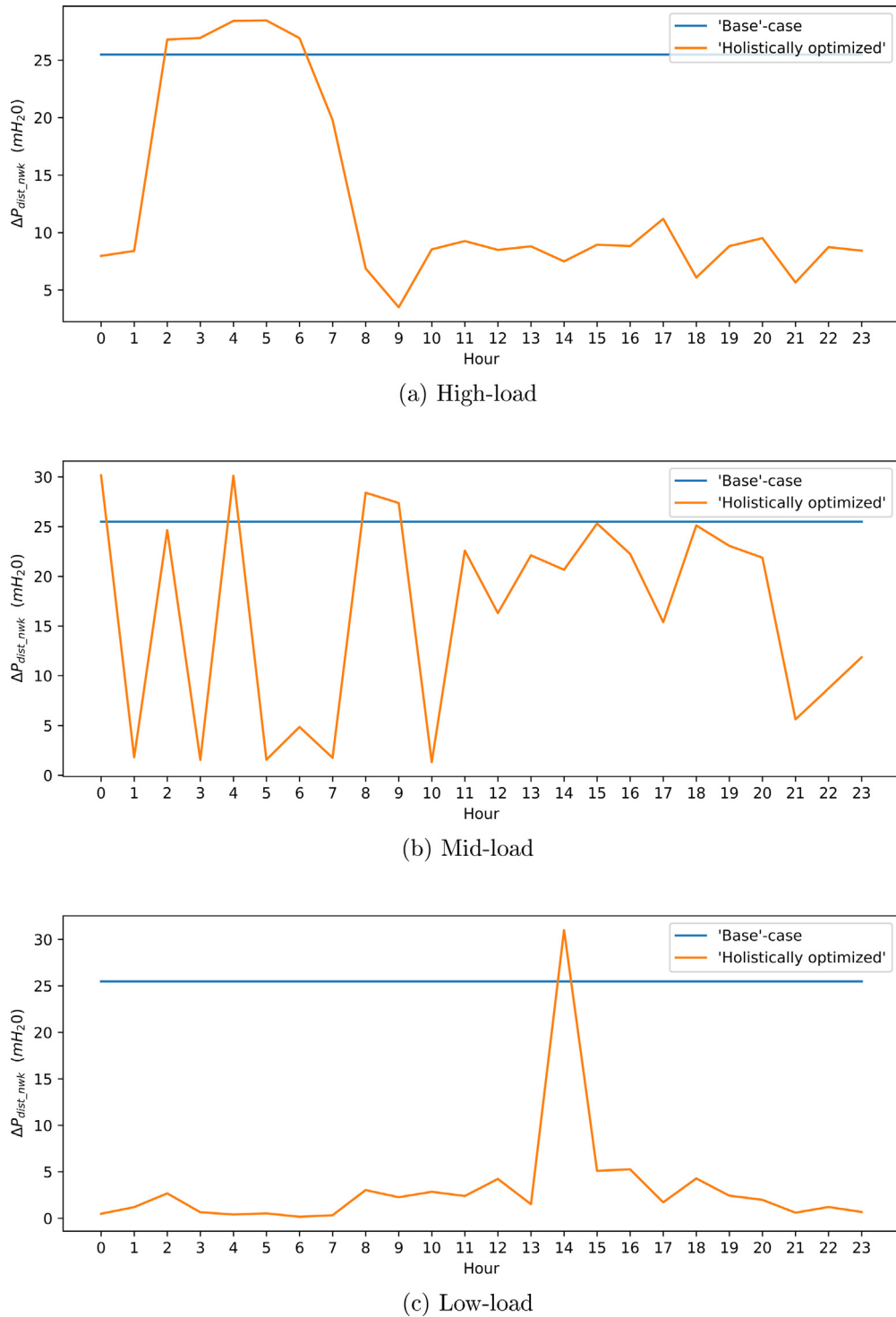


Fig. 5.6. Comparison of  $\Delta P_{dist\_nwk}$  between the 'base' and 'holistically optimized' cases.

the addition of a smaller chiller, storage or making changes to heat-exchangers at the substations could prove much more beneficial. Such conclusions could only be reached after conducting proper cost-benefit analyses.

## 6. Conclusion

District cooling systems have much to offer in terms of providing an energy efficient method of cooling production. Centralization of this process enables alternative energy sources to be easily integrated to fuel

the production, further enhancing energy efficiencies. The reality, however, is usually quite different owing to limited information available during the planning of the system. To account for this deficit in performance, an optimization framework for district cooling systems was proposed in this paper. It is meant to be used as a decision-making tool to guide design and operation of any given system of similar type.

Optimization studies in related fields are often highly simplified and do not reflect the issues encountered during operations. Component level optimization, neglecting the influence of varying chiller efficiencies and working fluid temperatures were some of the shortcomings

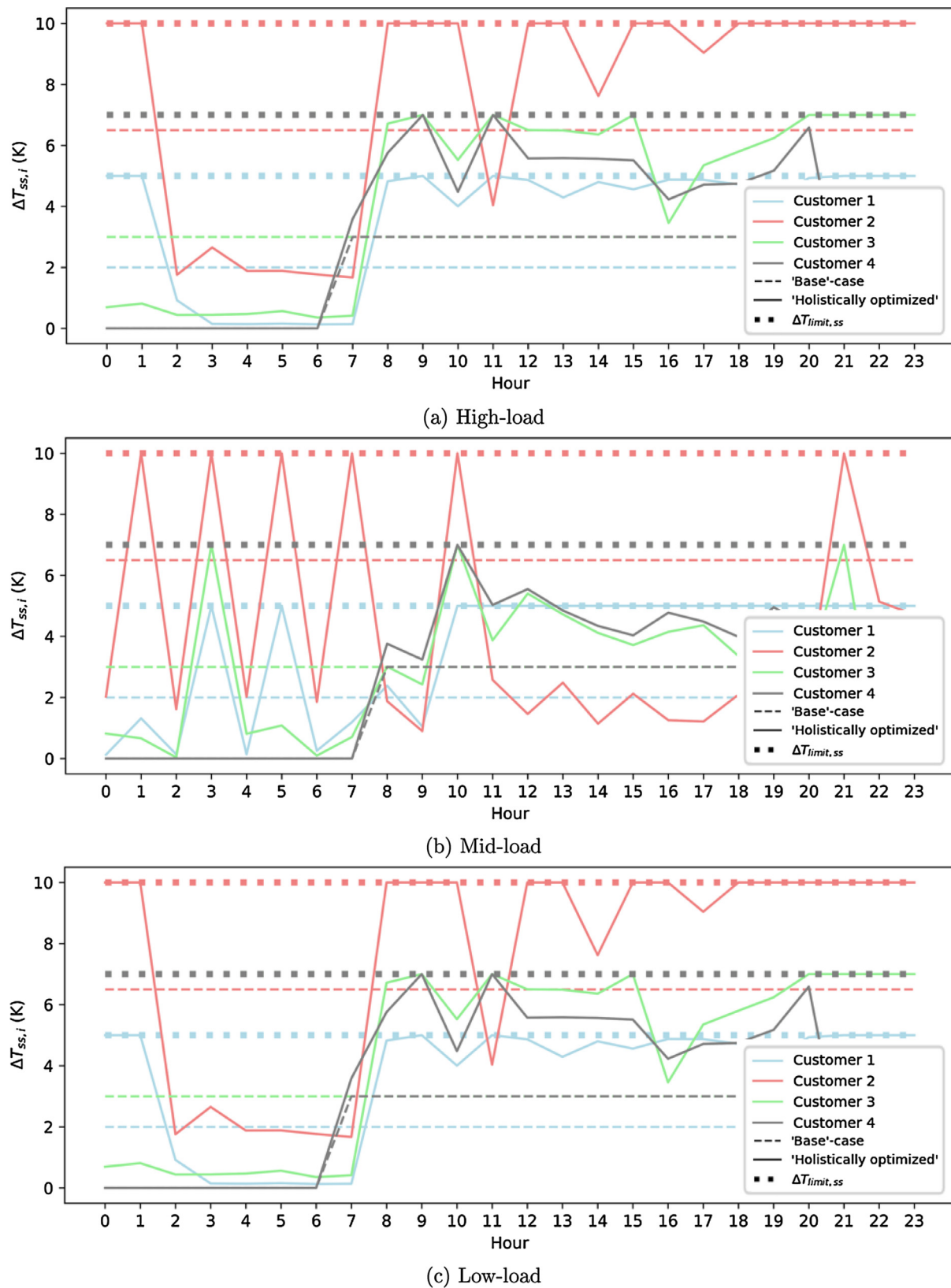


Fig. 5.7. Comparison of customer substation  $\Delta T$  between the 'base' and 'holistically optimized' cases.

addressed by the developed framework. This was done through the careful selection of models, model simplification and optimization techniques which allowed system level optimization to be performed with reasonable resolution time. For the problem discussed in the case

study, it took approximately 3-5 s to solve the mixed integer linear program sub-problem. The total resolution time of the optimization strategy depended on the stopping criterion defined for the genetic algorithm.

Finally, the capabilities of the optimization framework were illustrated through its application based on an existing cooling system. Investigation of the solutions generated gave insight into possible changes in operation and design which could improve energy efficiency. Electricity savings of up to 31% could potentially be realized under those conditions.

Further inclusion of essential features such as thermal storages and incorporation of load prediction modules would make the framework more comprehensive. These limitations form the basis for the future work to be embarked.

## Acknowledgments

The authors would like to acknowledge Veolia City Modeling Centre (VECMC) for the financial support.

## Appendix A. Supplementary material

Supplementary data associated with this article can be found, in the online version, at <https://doi.org/10.1016/j.apenergy.2019.01.134>.

## References

- [1] International Energy Agency. 2017 Key World Energy Statistics, International Energy Agency; 2017.
- [2] BP Statistical Review of World Energy, “BP statistical review of world energy june 2017,” Whitehouse associates, London; 2017.
- [3] Lindberg E. Six myths about climate change that liberals rarely question. *Transition Milwaukee* 2014.
- [4] Colourcoil Industries Sdn. Bhd., Colourcoil,” 2011. [Online]. Available: <<http://www.colourcoil.com/enewsvol6issue5/enews.htm>> [accessed 27 11 2015].
- [5] Henley J. World set to use more energy for cooling than heating. *The Guardian* 2015.
- [6] Cox S. Cooling a warming planet: A global air conditioning surge,” environment360; 2012.
- [7] Electrical and Mechanical Services Department, HKSARG. (25, 07 2014). Energyland. Retrieved 01 28, 2018, from <[http://www.energyland.emsd.gov.hk/en/building/district\\_cooling\\_sys/dcs\\_benefits.html](http://www.energyland.emsd.gov.hk/en/building/district_cooling_sys/dcs_benefits.html)> .
- [8] Uy HJ. District cooling is gaining momentum in Asia, Climate control middle east, Singapore; 2018.
- [9] Gulf F. Eco-Business,” 18 6 2014. [Online]. Available: <<http://www.eco-business.com/press-releases/understanding-and-unlocking-the-potential-of-district-cooling-in-asia/>> [accessed 19 4 2018].
- [10] Deng N, He G, Gao Y, Yang B, Zhao J, He S, et al. Comparative analysis of optimal operation strategies for district heating and cooling system based on design and actual load. *Appl Energy* 2017;205:577–88.
- [11] Schwelder M. Using low-load chillers to improve system efficiency. *ASHRAE J* 2017;14–20.
- [12] Yan C, Gang W, Niu X, Peng X, Wang S. Quantitative evaluation of the impact of building load characteristics on energy performance of district cooling systems. *Appl Energy* 2017;205:635–43.
- [13] Wang SW. Intelligent buildings and building automation. U.K: Taylor & Francis; 2009.
- [14] Jayamaha L. Energy-efficient building systems: green strategies for operation and maintenance. U.S.A.: McGraw-Hill Professional; 2006.
- [15] Gang W, Wang S, Xiao F, Gao D-c. District cooling systems: technology integration, system optimization, challenges and opportunities for applications. *Renew Sustain Energy Rev* 2016;53:253–64.
- [16] Fazlollahi S, Becker G, Ashouri A, Maréchal F. Multi-objective, multi-period optimization of district energy systems: IV - a case study. *Energy* 2015;84:365–81.
- [17] Ameri M, Besharati Z. Optimal design and operation of district heating and cooling networks with CCHP systems in a residential complex. *Energy Build* 2016;110:135–48.
- [18] Sameti M, Haghishat F. A two-level multi-objective optimization for simultaneous design and scheduling of a district energy system. *Appl Energy* 2017;208:1053–70.
- [19] Powell KM, Cole WJ, Ekarika UF, Edgar TF. Optimal chiller loading in a district cooling system with thermal energy storage. *Energy* 2013;50:445–53.
- [20] Schweiger G, Larsson P-O, Magnusson F, Lauenburg P, Velut S. District heating and cooling systems – framework for Modelica-based simulation and dynamic optimization. *Energy* 2017;137:566–78.
- [21] Jing ZX, Jiang XS, Wu QH, Tang WH, Huo B. Modelling and optimal operation of a small-scale integrated energy based district heating and cooling system. *Energy* 2014;73:399–415.
- [22] Sameti M, Haghishat F. Optimization approaches in district heating and cooling thermal network. *Energy Build* 2017;140:121–30.
- [23] Sakawa M, Katagiri H, Matsui T, Ishimaru K, Ushiro S. Long-term operation planning of district heating and cooling plants with contract violation penalties. *Scient Math Japon Online* 2010;411–20.
- [24] Skagestad B, Mildenstein P. District heating and cooling connection handbook. International Energy Agency; 1999.
- [25] Askarzadeh A, Coelho LdS. Using two improved particle swarm optimization variants for optimization of daily electrical power consumption in multi-chiller systems. *Appl Therm Eng* 2015;89:640–6.
- [26] Chang Y-C, Chan T-S, Lee W-S. Economic dispatch of chiller plant by gradient method for saving energy. *Appl Energy* 2010;87:1096–101.
- [27] Thangavelu SR, Myat A, Khambadkone A. Energy optimization methodology of multi-chiller plant in commercial buildings. *Energy* 2017;123:64–76.
- [28] Wang L, Lee EW, Yuen RK. A practical approach to chiller plants' optimization. *Energy Build* 2018;169:332–43.
- [29] Gurobi Optimization, Inc., Gurobi Optimization; 2016. [Online]. Available: <<http://www.gurobi.com>> [accessed 16 5 2018].
- [30] Gordon JM, Ng KC. Cool thermodynamics. Cambridge: Cambridge International Science Publishing; 2000.
- [31] Swider DJ. A comparison of empirically based steady-state models for vapor-compression liquid chillers. *Appl Therm Eng* 2003;23(5):539–56.
- [32] Lee T-S, Lu W-C. An evaluation of empirically-based models for predicting energy performance of vapor-compression water chillers. *Appl Energy* 2010;87:3486–93.
- [33] Wang Y, Jin X, Du Z, Zhu X. Evaluation of operation performance of a multi-chiller using a data-based chiller model. *Energy Build* 2018;172:1–9.
- [34] Wang H. A steady-state empirical model for evaluating energy efficient performance of centrifugal water chillers. *Energy Build* 2017;154:415–29.
- [35] Sherali HD, Alameddine A. A new reformulation-linearization technique for bilinear programming problems. *J Global Optim* 1992;2:379–410.
- [36] White FM. Fluid mechanics. New England: McGraw-Hill; 2009. (456) 347–.
- [37] Nonnenmann JJ. Chilled water plant pumping schemes, Stanley Consultants, Inc., Iowa.
- [38] M. Zakeer, Low delta-t syndrome in constant primary and variable secondary water system (Linkedin article),” 7 8 2015. [Online]. Available: <<https://www.linkedin.com/pulse/low-delta-syndrome-constant-primary-variable-zakeer>> [accessed 1 3 2018].
- [39] Marchi A, Simpson A. Evaluating the approximation of affinity laws and improving the estimate of the efficiency for variable speed pumping. *J Water Resour Plan Manage* 2013;139(12):1314–7.
- [40] Lu L, Cai W. A universal engineering model for cooling towers. International refrigeration and air conditioning conference, Indiana. 2002.
- [41] Viljoen J, Muller C, Craig I. Dynamic modeling of induced draft cooling towers with parallel heat exchangers, pumps and cooling water network. *J Process Control* 2018;68:34–51.
- [42] Ponce-Ortega JM, Serna-González M, Jiménez-Gutiérrez A. Optimization model for re-circulating cooling water systems. *Comput Chem Eng* 2010;34:177–95.